Investigation of the stoichiometry of MBE-grown Fe3O4 layers by magneto-optical Kerr spectroscopy

ELSEVIER

Thin Solid Films 292 (1997) 270–276

thin solid films

Investigation of the stoichiometry of MBE-grown Fe_3O_4 layers by magneto-optical Kerr spectroscopy

W.F.J. Fontijn [a], R.M. Wolf [a], R. Metselaar [b], P.J. van der Zaag [a,*]

[a] *Philips Research Laboratories, Prof. Holstlaan 4, 5656 AA Eindhoven, The Netherlands*

[b] *Department of Chemistry, Eindhoven University of Technology, P.O. Box 513, 5600 MB Eindhoven, The Netherlands*

Received 14 November 1995; accepted 25 April 1996

Abstract

The polar Kerr spectra between 0.7 and 4.0 eV of single-crystalline layers of Fe_3O_4 grown epitaxially on $MgAl_2O_4$, $SrTiO_3$ and MgO (100) substrates by means of oxidic molecular beam epitaxy are compared to the spectrum of a bulk synthetic single crystal of magnetite to asses the stoichiometry of the layers. Model calculations of the magneto-optical spectra of thin layers are used to explain the differences between the spectra of bulk Fe_3O_4 and thin layers of Fe_3O_4. The observed differences are attributed to interference effects and oxidation of the surface of the thin layers. The results are compared to magnetisation and Verwey transition data.

Keywords: Iron oxide; Magnetic properties and measurements; Molecular beam epitaxy; Surface composition

1. Introduction

As a result of improved deposition techniques the interest in oxidic magnetic thin layers for various applications has increased recently. Determining the stoichiometry of these layers, especially the oxygen concentration, is difficult. Due to the small sample volume chemical analysis is unsuitable. Furthermore, distinguishing between the layer and the, in comparison, huge substrate is difficult, especially in the case of epitaxial growth on an oxidic substrate.

One of the layer materials currently under investigation is magnetite, Fe_3O_4, [1–3]. Determining the stoichiometry of thin layers of Fe_3O_4 is especially complicated. Magnetite crystallizes in the inverse spinel structure, with cation distribution $(Fe^{3+})[Fe^{3+}Fe^{2+}]O_4$. In this structural formula the parentheses denote tetrahedral (A) sites and the square brackets denote the octahedral (B) sites. The iron is present in two ionisation states and the correlation time for electron hopping between $[Fe^{2+}]$ and $[Fe^{3+}]$, both on the octahedral sublattice, is 0.81 ps [4]. As a result, commonly used micro-analytical techniques such as Rutherford backscattering spectroscopy (RBS), X-ray photo-electron spectroscopy (XPS), electron probe microanalysis (EPMA) and Auger electron spectroscopy (AES) are not suitable since these techniques cannot distinguish between the iron ions and are relatively insensitive to oxygen [5]. As for depth profiling, EPMA is unsuitable and XPS and AES can only be used to this end in combination with sputtering. A potentially relatively accurate, however, also a comparatively complicated method to asses layer stoichiometry is conversion electron Mössbauer spectroscopy (CEMS) [3,6].

More indirect methods to estimate the stoichiometry of thin Fe_3O_4 layers, based upon the magnetic properties of Fe_3O_4, are the determination of the saturation magnetisation M_s [1] and the examination of the Verwey transition [2,3,7]. The saturation magnetisation M_s, however, provides an estimate with a large margin of error and may be subject to finite scaling effects. As for the Verwey transition, although the Verwey temperature, T_v, is very sensitive to deviations in stoichiometry, the suitability of T_v determination to establish the stoichiometry is limited. In thin layers a difference in expansion coefficient between layer and substrate may upset this determination. Furthermore, the determination of M_s and T_v are both unsuitable to obtain depth-dependent information concerning variations of stoichiometry.

Here, we present the results of an investigation into the suitability of Kerr spectroscopy to determine the quality of thin Fe_3O_4 layers. The prime advantage of Kerr spectroscopy is that this technique is only sensitive to the magnetic layer and insensitive to the substrate. Furthermore, four of the seven main magneto-optical (MO) transitions between 0.5 and 4.0 eV in Fe_3O_4 depend strongly on the Fe^{2+} concentration and are more or less evenly distributed over this energy

* Corresponding author.

PII S0040-6090(96)08910-9

interval [8]. This, combined with the fact that the penetration depth in Fe_3O_4 depends strongly on the wavelength (see below), makes depth-dependent analysis possible.

The aim of this paper is to explain the differences between the polar Kerr spectra of bulk Fe_3O_4 and (oxidic MBE grown) thin layers of Fe_3O_4. Using the data obtained for the bulk systems the possible contamination of the layers with substrate ions is investigated as well as the influence of interference. Also, the results are compared to the results of magnetisation measurements and an investigation of the Verwey transition.

2. Theoretical background

If the degeneracy of the orbital quantum number m_l of electronic transitions is lifted in a magnetic material due to spin–orbit coupling, optical anisotropy will be introduced. Consequently, the off-diagonal elements of the dielectric tensor are non-zero and MO Kerr effects are observed. The polar Kerr effect is the change in the polarisation state of a light beam which is reflected at normal incidence on a perpendicularly magnetized sample. The Kerr rotation θ_k is related to the change in the phase and the Kerr ellipticity ϵ_k to the change in amplitude. To a first approximation the Kerr effect depends linearly on the magnetisation [9].

For a crystal with cubic symmetry, magnetized perpendicular to the surface, i.e. along the z direction, the dielectric tensor can be written in the form:

$$\tilde{\varepsilon} = \begin{vmatrix} \tilde{\varepsilon}_{xx} & \tilde{\varepsilon}_{xy} & 0 \\ -\tilde{\varepsilon}_{xy} & \tilde{\varepsilon}_{xx} & 0 \\ 0 & 0 & \tilde{\varepsilon}_{zz} \end{vmatrix} \quad (1)$$

with $\tilde{\varepsilon}_{xx} = \varepsilon'_{xx} + i\varepsilon''_{xx}$ and $\tilde{\varepsilon}_{xy} = \varepsilon_{xy}' + i\varepsilon_{xy}''$ if the sign convention of Reim and Schoenes is followed [10]. The elements of the dielectric tensor can be expressed in the observables n, k, θ_k and ϵ_k, the refractive index, the absorption index and the Kerr rotation and elipticity respectively. For the polar Kerr effect [10]:

$$\begin{aligned} &\varepsilon'_{xx} = n^2 - k^2, \quad \varepsilon''_{xx} = 2nk \\ &\varepsilon'_{xy} = A \cdot \theta_k - B \cdot \epsilon_k \\ &\varepsilon''_{xy} = -B \cdot \theta_k - A \cdot \epsilon_k \end{aligned} \quad (2)$$

with $A = (n^3 - 3nk^2 - n)$ and $B = (-k^3 + 3n^2)$.

The Kerr effect signal stems primarily (for 99.6%) from about twice the penetration depth of the light, d_p. This depth is by definition the depth for which the intensity of the light is reduced with a factor e^{-1}. Hence, $d_p = \lambda/(4\pi k)$, with k the absorption index and λ the wavelength. As a result the Kerr effect yields surface-sensitive information for samples much thicker than d_p.

For samples with thicknesses in the order of d_p multiple reflections can occur. In the following description of the resulting interference, the Kerr and Faraday ellipticity are neglected for reasons of clarity and a distinction is made between θ_k, the intrinsic Kerr rotation, and θ, the effective rotation. In Fig. 1(a) two separate light paths are depicted. One corresponding to $E_{r,1}$, the result of normal reflection at the surface and one corresponding to $E_{r,2}$, the result of reflection at the interface between the MO layer and the substrate. The incident light vector, E_{in}, is taken linearly polarized along the y axis (the actual angle of incidence is much smaller than in the figure). Upon reflection at the surface of the perpendicularly magnetized layer, a small x component is introduced in the polarisation state of $E_{r,1}$ due to the Kerr effect. In thick layers and bulk samples this yields E_{out} (Fig. 1(b)), exhibiting Θ_k. The length of the vector E_{out} is smaller than E_{in} due to a certain amount of absorption and transmission. In thin layers the two light vectors, $E_{r,1}$ and $E_{r,2}$, interfere with each other. The phase and amplitude of $E_{r,2}$ depend on the layer thickness, the wavelength, the dielectric tensor of layer and the refractive index of the substrate. Adding the two light vectors, ignoring multiple reflections in this description, results in E_{out} (Fig. 1(c)), which shows increased or decreased rotation, Θ, depending on the phase of $E_{r,2}$. For a complete quantitative description see Ref. [11].

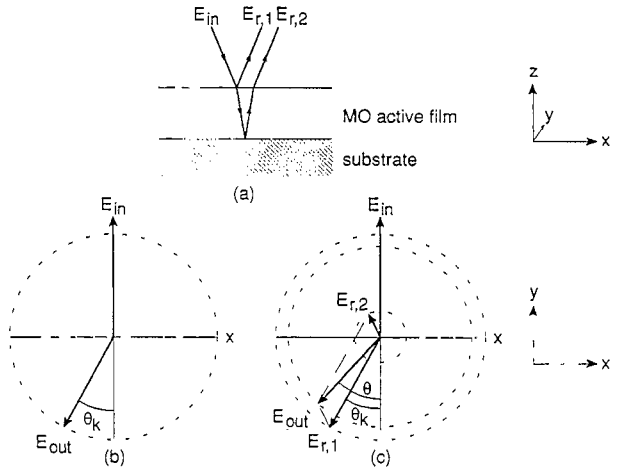

Fig. 1. Schematic diagram of the effect of interference on the measured Kerr rotation (see text for details).

3. Experimental procedures

3.1. Sample preparation and apparatus

Single-crystalline thin layers of Fe_3O_4 were deposited by oxidic molecular beam epitaxy (oxidic MBE) on the (100) face of various substrates: $MgAl_2O_4$, with spinel-type structure and a lattice mismatch of 3.9% with respect to Fe_3O_4, $SrTiO_3$, with perovskite-type structure and a lattice mismatch of 7.5% and MgO, with rocksalt-type structure and a lattice mismatch of 0.35% (A list of the thin film samples studied is given in Table 1). The MBE apparatus used is a differentially pumped Balzers UMS630 MBE equipped with three e^--guns, three Knudsen cells, and a mass spectrometer controlled evaporation flux with a fast (1 ms) feedback sys-

Table 1

d (nm)	Substrate	M_s (kA m^{-1})	$a_\perp$ (Å)	T_v (K)	t' (nm)	Fig.
40	$MgAl_2O4$	429	8.380 ± 0.004	107 ± 1	4	–
115	$MgAl_2O_4$	457	8.398 ± 0.004	109 ± 1	3.5	5
360	$MgAl_2O_4$	473	8.396 ± 0.004	122 ± 1	1.5	2, 3
100	$SrTiO_3$	nd	8.391 ± 0.004	nd	3.5	5
100	MgO	nd	8.360 ± 0.004	98 ± 2	nd	–
Bulk	–	480	8.396	122	–	2

The single-crystalline layers of Fe_3O_4 studied their saturation magnetisation, M_s (at 293 K), perpendicular lattice parameter, $a_\perp$, Verwey temperature, T_v, and the calculated thickness of the oxidized part of the layer, t'. All layers were epitaxially grown on (100) substrates (growth direction [100]).(nd = not determined)

tem. The films were deposited at 300 °C at a partial oxygen pressure in the 10^{-3} Pa range. The oxygen pressure determines the degree of oxidation of the iron [12]. By means of X-ray diffraction (XRD) the lattice parameters (θ–2θ scans) and the degree of crystallographic quality of the layers were verified. X-ray fluorescence (XRF) was used to determine the layer thicknesses, with an accuracy of 5%. The saturation magnetisation, M_s, of the Fe_3O_4 layers was determined by SQUID magnetometery (Quantum Design, MPMS5) at 293 K. The Verwey transition was determined through resistivity measurements.

The polar Kerr spectra of the thin Fe_3O_4 layers between 0.7 and 4.0 eV (1700–310 nm) were measured on the following apparatus. Light from a 450 W Xe arc lamp (Osram XBO) is focused with a set of mirrors on the entrance slit of a monochromator (SPEX 1702). The beam from the monochromator passes a filter (to attenuate the higher order reflections), a Glan–Thompson polarizer, a photo-elastic modulator (Hinds CF5) and a lens which focuses the light on the sample, situated between the poles of a 1400 kA m^{-1} water-cooled electromagnet. After reflection from the sample, the light passes through a lens, a chopper and an analyzer before reaching the detector. This is either a Ge photodiode (Rofin 7460) for the 0.7–1.4 eV range or a photomultiplier (Hamamatsu R943-02) for the 1.4–4.0 eV range. The detector signal was pre-amplified (current to voltage) and fed into three lock-in amplifiers (EG&G 5209, 5205 and 5207) to measure the light intensity, rotation and ellipticity. The set-up is controlled by a Hewlett Packard computer (HP-300). This apparatus is similar to the one described by Martens et al. [13]. A detailed description of the technique for the measurement of the Kerr rotation using a photo-elastic modulator has been given by Sato [14]. θ_k and ϵ_k were measured at ambient temperature, with a saturating magnetic field applied perpendicularly to the sample surface ($H = 1400$ kA m^{-1}). By averaging measurements in opposite field directions any offset in Kerr amplitude is eliminated. More details on the Kerr spectrometer and measurement procedure can be found elsewhere [15].

3.2. Model calculations

The polar Kerr spectra of the magnetite thin films were calculated, using the dielectric tensors of bulk samples. These model calculations were carried out with a program based on the method described in Ref. [11]. The diagonal and off-diagonal elements of the dielectric tensor of pure and substituted magnetite had been determined earlier [8]. The substrates were assumed to have zero absorption and an infinite thickness. Thus, only the spectral dependence of the substrates refractive index was taken into account, as obtained from the literature ($MgAl_2O_4$ [16], $SrTiO_3$ [17]).

To fit the calculated to the measured spectra of the thin Fe_3O_4 layers, the effect of contamination of the layers by the $MgAl_2O_4$ substrate ions was investigated. The following configurations were investigated: a homogeneous distribution of substrate metal ions inside the layer, the presence of either Mg^{2+}, Al^{3+} or both at the top or at the layer–substrate interface. These configurations were tested in the calculations by replacing in the parts of the layer concerned the off-diagonal element of the dielectric tensor of Fe_3O_4 by the off-diagonal element of the Mg^{2+} and, or Al^{3+} substituted bulk samples [8]. The use of the same diagonal elements in all the calculations ensured that no artificial interfaces were introduced.

The fit procedure described above is fairly complicated. By using the results of the first fit procedure and assuming the influence of interference only to depend on the layer thickness, it is possible to devise a second, less complicated fit procedure by fitting the Kerr spectrum directly. This second procedure is based on a model with three layers of which the first two have variable thicknesses, t' and t'' respectively. The thickness of the third layer follows from the actual thickness of the layer, t, of which the Kerr spectrum is to be fitted, minus the combined thickness of the first two layers in the model. For the Kerr spectrum of the first layer the spectrum of $Mg_{0.8}Fe_{2.2}O_4$ is taken, for the second layer the spectrum of $Al_{0.005}Fe_{2.995}O_4$ and for the third the spectrum of pure Fe_3O_4. Of each layer in the model the relative contribution to the measured Kerr effect as a function of depth is calculated from the absorption index. Subsequently, the Kerr spectrum of the model is calculated by taking the algebraic sum of the contribution of each layer of the model and the calculated interference for a layer with the actual thickness of the layer to be fitted. The calculated interference follows from subtracting the Kerr spectrum of bulk Fe_3O_4 from the calculated spectrum of a perfect layer. The linear additivity of the Kerr

effect is a first order approximation which is at least valid if $2\pi/\lambda \cdot tn \ll 1$, as demonstrated by Zak et al. [18]. This second model is optimized by determining the model layer thicknesses for which the closest fit to the measured spectrum is achieved.

4. Results and discussion

In Fig. 2 the magneto-optical (MO) polar Kerr spectra are shown of bulk Fe_3O_4 and of a 360 nm thick layer of Fe_3O_4 epitaxially grown (growth direction [100]) by oxidic MBE on a $MgAl_2O_4$ (100) substrate. The MO Kerr spectrum of bulk Fe_3O_4 is taken from Ref. [8]. As can be seen in Fig. 2, the magneto-optical polar Kerr spectrum of the Fe_3O_4 layer differs considerably from the bulk Fe_3O_4 spectrum. Before it can be determined whether or not stoichiometric deviations are, at least partly, responsible for the observed differences, possible interference effects have to be isolated. To this end, the model calculations proved to be a useful tool in separating the interference effects from true changes in the dielectric tensor. In Fig. 3 the MO spectra of Fe_3O_4 layers are shown, calculated from the dielectric tensor of Fe_3O_4 (Fig. 3(a)) and of substituted Fe_3O_4 (Fig. 3(b)). The calculations show that optical interference is responsible for the observed differences between the spectra of bulk and the thin Fe_3O_4 layer in the region below 2.2 eV.

Fig. 4 shows the penetration depth d_p versus photon energy for Fe_3O_4 as derived from previously obtained data [8]. Three regions can be identified. Between 0.8 and 2.0 eV, d_p is relatively large with a maximum at 1.35 eV of 159 nm, between 2.0 and 3.0 eV d_p is gradually decreasing, and between 3.0 and 4.0 eV d_p is relatively small (35–25 nm). This behaviour results from the strong intervalence charge transfer (IVCT) transition at 0.55 eV in combination with the onset, around 2.0 eV, of a very strong and broad absorption band centred around 6 eV [19]. Consequently, especially the Kerr spectrum in the first region is influenced by interference, whereas the last region yields the most surface-sensitive information.

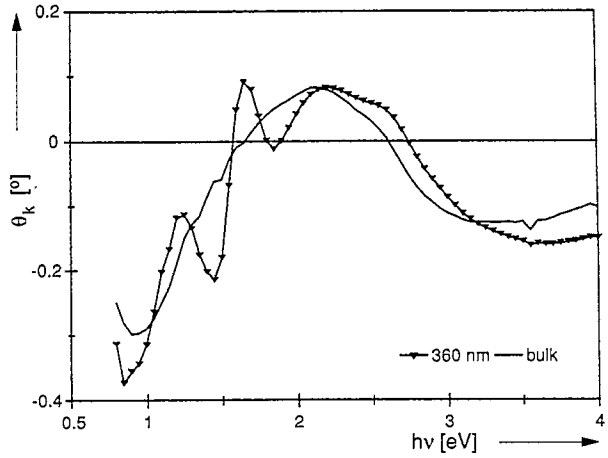

Fig. 2. The MO Kerr rotation spectrum of bulk Fe_3O_4 (———) compared to the spectrum of a 360 nm thick Fe_3O_4 layer grown epitaxially on $MgAl_2O_4$ (100) (▼).

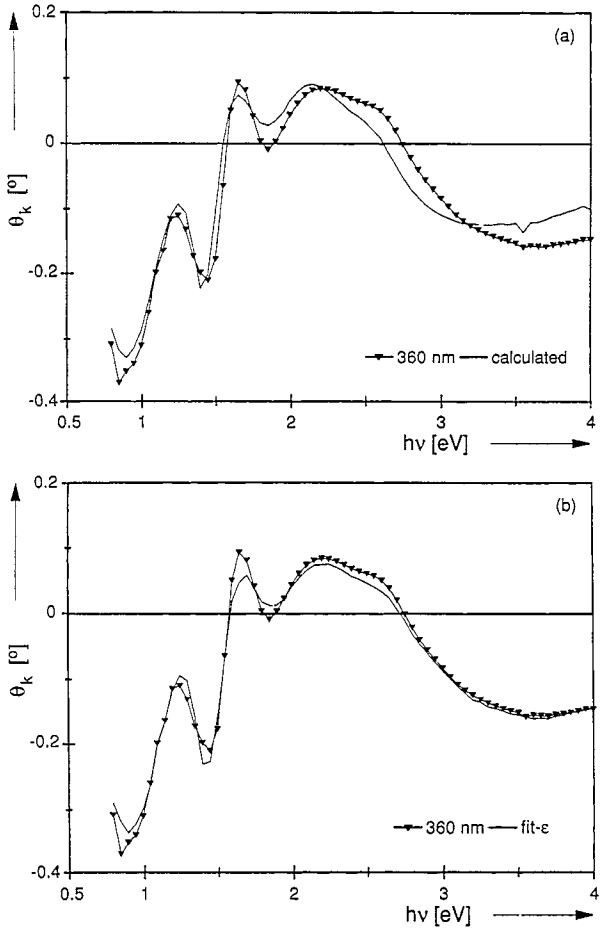

Fig. 3. The measured Kerr rotation spectrum of a 360 nm thick Fe_3O_4 layer (▼) compared to (a) the calculated spectrum of this layer using the dielectric tensor of bulk Fe_3O_4 (———); (b) the fit of the spectrum of this layer using the dielectric tensors of bulk and substituted Fe_3O_4 (———) (see text for details).

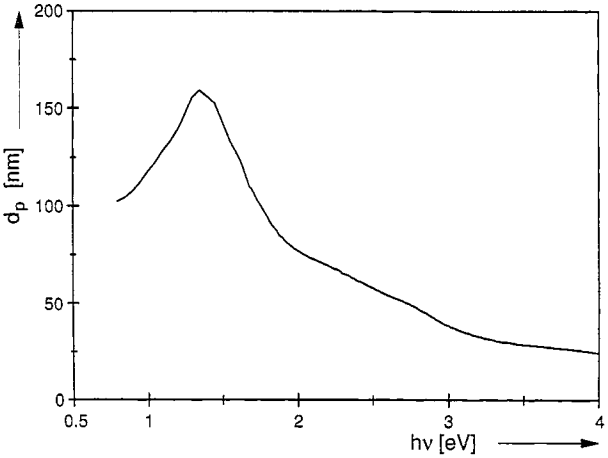

Fig. 4. The penetration depth, d_p, in213 Fe_3O_4 versus the photon energy calculated from the optical data of Fe_3O_4 [8].

Above 2.2 eV the calculated rotation for a 360 nm thick layer (——— in Fig. 3(a)) is identical to the measured

rotation for bulk Fe_3O_4 (——— in Fig. 2). Thus, above 2.2 eV $E_{r,2}$, and consequently the interference, is negligible. Moreover, as d_p is 70 nm at 2.2 eV, we can conclude that significant interference only occurs if $t < 5d_p$. Model calculations confirm this threshold, since the maximum penetration depth in the photon energy range considered here is 159 nm (see Fig. 4) and the calculated interference is negligible for layers thicker than 800 nm.

In Fig. 3(a) we observe that interference effects cannot fully explain the measured thin layer spectrum. The calculated rotation fits the rotation of the measured thin layer below 1.75 eV. However, at higher energies differences still persist, possibly as a result of stoichiometric deviations. The fact that the persisting differences are predominantly in the higher energy range ($h\nu > 2$ eV) indicates that the possible stoichiometric deviations in the thin layer are mainly limited to the top of the layer (compare Fig. 4). This conclusion is confirmed by the fact that the calculated spectra of layers with varying amounts of Mg^{2+} and/or Al^{3+} at the interface between layer and substrate did not yield an improved fit to the measured rotation spectrum while placing Mg^{2+} and Al^{3+} on top did.

The closest match to the measured spectrum of the thin layer was achieved by assuming both Mg^{2+} (thickness, 20 nm; atomic fraction, 0.2) and Al^{3+} (thickness, 150 nm; atomic fraction, 0.005) to be present at the top of the layer. Using such a model for the top layer of the Fe_3O_4 film results in the calculated spectrum shown in Fig. 3(b). Note the in comparison to Fig. 3(a) much better agreement with the measured spectrum above 2.2 eV.

However, Mg^{2+} could not be found inside the layers with other techniques (XPS/RBS) while the 0.005 Al^{3+} content is too small to be detected. Furthermore, the differences between calculated and measured MO spectra are quite similar for the 115 nm thick layer on $MgAl_2O_4$ and the 100 nm thick layers deposited on $SrTiO_3$ (see Fig. 5) and MgO. Therefore, we can exclude the possibility that contamination the Fe_3O_4 layer with Mg^{2+} or Al^{3+} ions from the substrate is responsible for the deviations in the spectrum. As Mg^{2+} and Al^{3+} are both diamagnetic ions, they do not give rise to additional transitions in the MO spectrum. These ions merely substitute [Fe^{2+}] and [Fe^{3+}], respectively, decreasing the intensities of the IVCT transitions [8]. In addition, they alter the lattice parameter locally, changing the energies at which the IVCT transitions take place [8]. Changing the composition and (or) the lattice by other means, for instance by reduction or oxidation, exhibits similar effects. For example, between 2.0 and 4.0 eV the spectrum appears to be shifted to a higher energy for the measured layer compared to the calculated layer in Fig. 3(a). A similar shift in energy, however, for the complete spectrum, is observed when [Fe^{3+}] is substituted by Al^{3+} [8]. This shift is caused by localised distortions introduced as a result of the relatively small radius of the Al^{3+} ion compared to the radius of the [Fe^{3+}] ion. Cation vacancies would result in similar distortions. Therefore, the most plausible explanation seems to be an oxidation of at least the top surface, resulting in cation vacancies and localized lattice distortions, perturbing the octahedral symmetry. In the calculations, the Mg^{2+} substitution then represents the loss of Fe^{2+} and Al^{3+} substitution represents the perturbation of the octahedral symmetry.

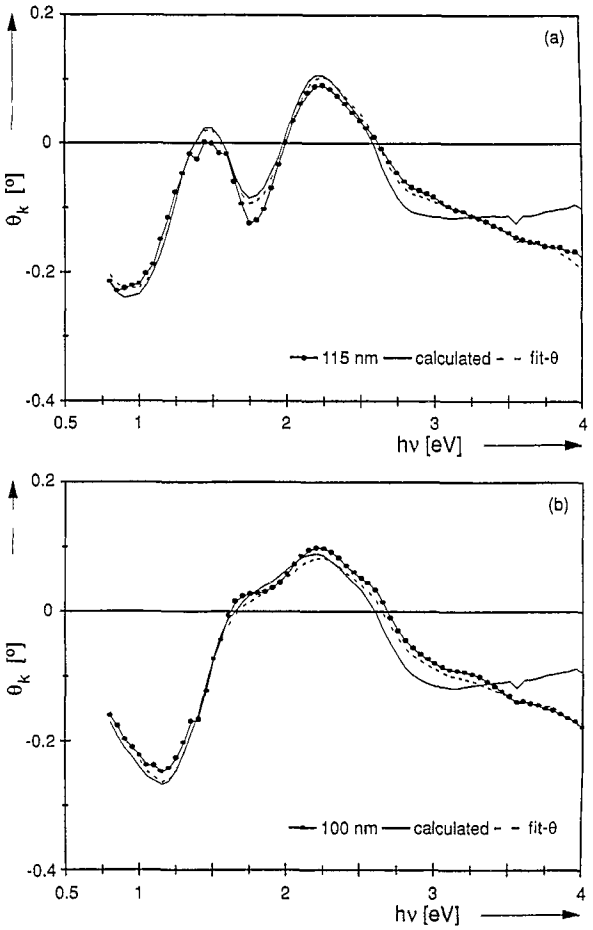

Fig. 5. Comparison of the measured Kerr rotation spectrum of (a) a 115 nm thick Fe_3O_4 layer on $MgAl_2O_4$ (–●–) and (b) of a 100 nm thick Fe_3O_4 layer on $SrTiO_3$ (–●–), to the calculated spectrum using the dielectric tensor of bulk Fe_3O_4 (———) and to the fit of this spectrum using the Kerr spectra of Fe_3O_4, $Al_{0.005}Fe_{2.995}O_4$ and $Mg_{0.8}Fe_{2.8}O_4$ (– – –) (see text for details).

To confirm the oxidation hypothesis we annealed the 360 nm thick Fe_3O_4 layer in air at 200 °C for 4 h, thus promoting oxidation of the top of the layer. Fig. 6 shows the MO Kerr spectrum of this layer after the annealing. We find that the characteristically smaller rotation around 3 eV for the 115 nm and 100 nm thick measured layers compared to the calculated perfect layers of the same thicknesses (Fig. 5) is also present in the annealed layer. This is due to a reduced intensity of the intervalence charge transfer transition (IVCT) $[Fe^{2+}]_{t2g} \rightarrow (Fe^{2+})_e$ at 3.11 eV [8]. The additional features in the spectrum between 3.0 and 4.0 eV, already visible in Fig. 5, are intersublattice charge transfer transitions which are no longer obscured by the IVCT transitions due to the higher degree of oxidation.

It is difficult to establish the exact degree of oxidation and the layer thickness involved. Partly because the oxidation

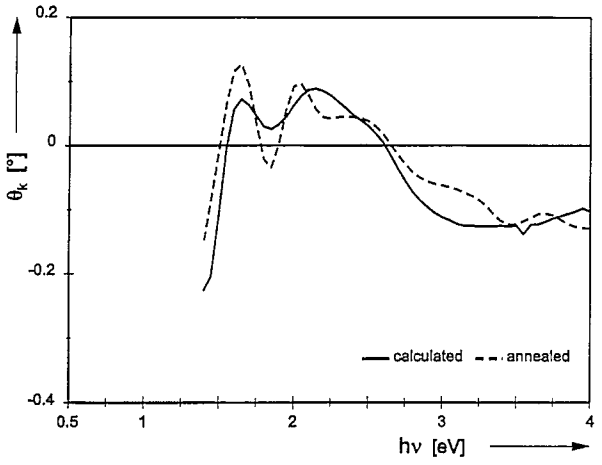

Fig. 6. The calculated Kerr rotation spectrum of a 360 nm thick Fe_3O_4 layer (———) compared to the measured spectrum after annealing in air at 200°C for 4 hours (– – –).

degree can not be expected to be constant inside the layer, and partly because the combination of Mg^{2+} and Al^{3+} can only approximate the effects of oxidation. Furthermore, the assumption that diagonal element of the dielectric tensor remains constant throughout the layer constitutes another approximation. However, it is possible to obtain a more accurate estimate of the oxidation degree by using the second fit procedure described in Section 3.2. The results of the fit are reported in Table 1. It should be noted that the resulting thickness for the top layer, t', is only an estimate. We may conclude, however, that the layer thickness involved in oxidation is in the order of a few (~ 3) nm. For the annealed layer a t' of 7 nm was found, further confirming our oxidation hypothesis. The thickness of the second model layer, t'', is in the order of 30–50 nm. This thickness may, however, have no real physical meaning other than that it is a measure for the additional shift in energy of the spectrum compared to Mg^{2+} substitution. As stated above Mg^{2+} only reproduces the loss of Fe^{2+} as a result of oxidation and not the change in lattice parameter accompanying oxidation since Mg^{2+} substitution has no major effect on the lattice parameter [20].

If we assume a non-contributing or "dead" layer with a thickness of the same order as the calculated t', we can correct M_s by taking into account this "dead" layer (multiply M_s by $1+t'/t$). We then find for the 360, 115 and 40 nm thick layers 475, 471 and 472 kA m^{-1} respectively, close to the bulk value of 480 kA m^{-1} [20]. Thus, the thickness found from the fits for the oxidized top layer, t', is consistent with the saturation magnetisation, M_s, reported in Table 1.

The temperature at which the Verwey transition occurs, T_v, is a good measure of the stoichiometry of bulk Fe_3O_4 [7]. As this property has also been applied previously to the study of Fe_3O_4 thin films [2], we determined T_v for the layers in our study. The Verwey temperatures given in Table 1 were determined from the resistivity, ρ, rather than the magnetisation as the former method is more sensitive. In our ρ vs. T data [21] we find no discontinuity, which poses a problem regarding the definition of T_v. In this study we have taken the temperature at which the derivative of ρ/T vs. T^{-1} is maximum as a measure for T_v. The results are presented in Table 1. The reduced T_v of the layers with respect to the T_v of bulk Fe_3O_4 could be accounted for by some oxidation of the total layers. For example, a T_v of 109 K would indicate, in case of a bulk sample, a δ of 0.012 [7], with δ defined by $Fe_{3-\delta}O_4$. However, in the case of epitaxially grown thin layers other effects have to be considered also, notably, the effect of epitaxial strain and strain due to differences between the thermal expansion coefficients of the Fe_3O_4 film and the substrate. The latter, since the Verwey transition occurs some 400 K below the growth temperature. We have argued elsewhere [21] that, in the case of the $MgAl_2O_4$ substrate, the differences in thermal expansion coefficients are the most likely cause for the observed reduction in T_v. Furthermore, in the case of the Fe_3O_4 film grown on the MgO substrate the largest shift in T_v is found: 25 K. For this sample epitaxial strain as a result of coherent growth, is relevant, as follows from the lattice parameter (see Table 1). Thus, although the reduced T_v data found for our films are not inconsistent with the conclusions of the analysis of the MO Kerr spectra, strain is also important. This suggests that in epitaxially grown Fe_3O_4 films a stoichiometry analysis based on T_v has to be exercised with care.

5. Conclusions

By using magneto-optical Kerr spectra in combination with model calculations and XPS/RBS measurements we have shown that it is possible to obtain valuable information concerning the stoichiometry and depth profiles throughout a thin ferrite layer; also the layer thickness can be estimated. From fits of the Kerr Spectra it is found that the top 2–4 nm surface layers of the films are oxidized, which is consistent with saturation magnetisation data.

Acknowledgements

It is a pleasure to thank H.W. van Kesteren for the stimulating discussions and R.J.M. van de Veerdonk for the resistivity measurements.

References

[1] P.A.A. van der Heijden, J.J. Hammink, P.J.H. Bloemen, R.M. Wolf, M.G. van Opstal, P.J. van der Zaag and W.J.M. de Jonge., *Mater. Res. Soc. Symp. Proc., 384* (1995) 27.
[2] E. Lochner, K.A. Shaw, R.C. DiBari, W. Portwine, P. Stoyonov, S.D. Berry and D.M. Lind, *IEEE Trans. Mag., 30* (1994) 4912.
[3] T. Fujii, M. Tanako, R. Katano, Y. Isozumi and Y. Bando, *J. Magn. Magn. Mater., 130* (1994) 267.
[4] T. Mizoguchi and M. Inoue, *J. Phys. Soc. Jpn., 21* (1966) 1310.
[5] L.C. Feldman and J.W. Mayer, *Fundamentals of Surface and Thin Film Analysis*, North-Holland, New York, 1986.

[6] F.C. Voogt, T. Hibma, G.L. Zhang, M. Hoefman and L. Niesen, *Surf. Sci., 331–333* (1995) 1508.
[7] J.P. Shepherd, J.W. Koenitzer, R. Aragón, J. Spałek and J.M. Honig, *Phys. Rev. B, 43* (1991) 8461.
[8] W.F.J. Fontijn, P.J. van der Zaag, M.A.C. Devillers, V.A.M. Brabers and R. Metselaar, *Phys. Rev. B*, submitted.
[9] F.J. Kahn, P.S. Pershan and J.P. Remeika, *Phys. Rev., 186* (1969) 891.
[10] W. Reim and J. Schoenes, Magneto optical spectroscopy of f-electron systems, in E.P. Wohlfarth and K.H.J. Buschow (eds.), *Handbook of Ferromagnetic Materials*, North-Holland, Amsterdam, 1990.
[11] M. Mansuripur, *J. Appl. Phys., 67* (1990) 6466.
[12] R.M. Wolf, A.E.M. Veirman, P. van der Sluis, P.J. van der Zaag and J.B.F. aan de Stegge, *Mater. Res. Soc. Symp. Proc., 341* (1994) 23.
[13] J.W.D. Martens, W.L. Peeters, P.Q.J. Nederpel and M. Erman, *J. Appl. Phys., 55* (1984) 1100.
[14] K. Sato, *Jpn. J. Appl. Phys., 20* (1981) 2403.
[15] W.B. Zeper, Magneto-optical recording media based on Co/Pt multilayers, *PhD Thesis*, University of Twente, Enschede, The Netherlands, 1991.
[16] S. Koritnig in Landolt and Börnstein (eds.), *Landolt–Börnstein*, Band II teil 8, Springer, Berlin, 1956–1971.
[17] G. Calsow, *J. Gemmology London, 5* (1955) 98.
[18] J. Zak, E.R. Moog, C. Liu and S.D. Bader, *J. Magn. Magn. Mater., 88* (1990) L261.
[19] X.X. Zhang, J. Schoenes, W. Reim and P. Wachter, *J. Phys. C: Solid State Phys., 16* (1983) 6055.
[20] J. Smit and H.P.J. Wijn, *Ferrites*, Philips Technical Library, Eindhoven, 1959.
[21] P.J. van der Zaag, W.F.J. Fontijn, P. Gaspard, R.M. Wolf, V.A.M. Brabers, R.J.M. van de Veerdonk and P.A.A. van der Heijden, *J. Appl. Phys., 79* (1996) 5936.